

Characterizing the Outburst of the Supermassive Black Hole in M87

William Forman¹, Eugene Churazov^{2,3}, Sebastian Heinz⁴,
Christine Jones¹, Paul Nulsen¹, Ralph Kraft¹, Scott Randall¹
and Alexey Vikhlinin^{1,3}

¹Harvard-Smithsonian Center for Astrophysics, 60 Garden St., Cambridge, MA, USA
email: wforman@cfa.harvard.edu

²MPA, Karl-Schwarzschild Strasse 1, 85748 Garching bei Munchen, Germany

³Space Research Institute, 84/32 Profsoyuznaya Str, Moscow, Russia

⁴University of Wisconsin, 4506 Sterling Hall, Madison, WI 53706 USA

Abstract. M87, in the Virgo cluster, allows us to study the interaction of a supermassive black hole (SMBH) with its hot gaseous atmosphere. Deep Chandra observations reveal a nearly circular shock front with a Mach number of 1.2 and a radius of 13 kpc which is driven by a central cavity inflated by an SMBH outburst began 12 million years ago. An outburst with an energy of $\sim 5 \times 57$ ergs and a duration of ~ 2 Myrs provides a good match to all the constraints. For an outburst repetition rate of about 12 Myrs (the outburst age), the outburst energy is sufficient to balance the radiative cooling of the gas. The outburst duration in M87 argues for a “gentle” (long duration) outburst that does not generate strong shocks and where much of the outburst energy is deposited in the cavities that then transfer energy to the surrounding gas as they buoyantly rise.

Keywords. supermassive black hole, cool core, AGN outburst

1. Chronicling the outburst history of the supermassive black hole in M87

Galaxies, groups and clusters form a family of dark matter halos. At the center of each of these halos that are filled with hot, X-ray emitting plasma, especially those referred to as cool core systems where the gas cooling time is short compared to the age of the system, there is generally a single massive galaxy with a supermassive black hole (SMBH) in the core. Fig. 1 shows three examples of hot gaseous atmospheres ranging from galaxy/group scales to the very massive cluster scale. In these examples, each X-ray atmosphere exhibits large cavities, which were produced by energetic outbursts from the central SMBH. Often, the only way to derive the total energy release from the SMBH is through the effects of the SMBH on its environment (e.g. the production of cavities and shocks in the surrounding X-ray emitting gas). While the accretion onto the SMBH appears to be radiatively inefficient at the present epoch, the mechanical output from these black hole outbursts is sufficient to inflate cavities with total energies ranging from 10^{56} ergs for individual galaxies to as high as 10^{62} ergs for the largest cavities seen in massive clusters (e.g. Finoguenov & Jones 2001; Fabian *et al.* 2003; McNamara *et al.* 2005; Churazov *et al.* 2002).

In this contribution, we focus on the X-ray and radio observations of M87 based on the work described in Churazov *et al.* (2001) and Forman *et al.* (2005, 2007, 2017) which provide more details. M87 lies at a distance of 16 Mpc and hosts a SMBH with a

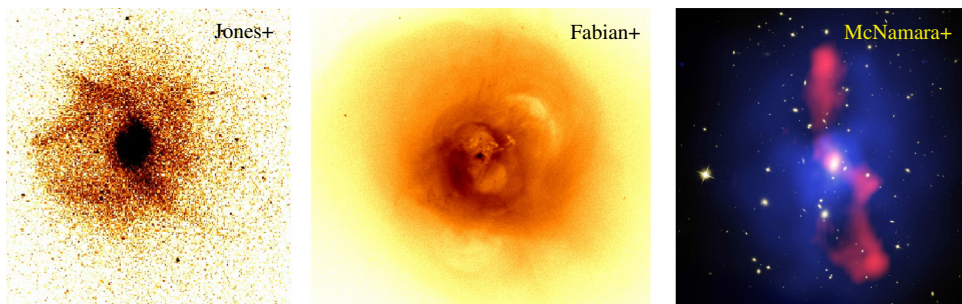


Figure 1. Early type galaxies, groups and clusters form a family of dark matter halos. As the halo mass increases, so does the baryon fraction, gas temperature, and X-ray luminosity. Many systems have strongly peaked X-ray surface brightness profiles that imply short gas cooling times and that are centered on a bright central galaxy (BCG). In the systems shown (from left to right, NGC4636, Perseus/NGC1275, MS0735), each X-ray atmosphere exhibits large cavities, which were produced by energetic outbursts from the central SMBH of the BCG.

mass of $3 - 6 \times 10^9 M_{\odot}$ (e.g. Ford *et al.* 1994; Walsh *et al.* 2013). The X-ray and radio observations of M87 chronicle the outbursts from the SMBH over the past 150 Myr (see Fig. 2 and 3). Fig. 2 (left panel) shows the broad band X-ray image of M87 including the jet (extending $20''$ from the nucleus to the NW) which is filling the central cavity with relativistic plasma clearly seen as the very dark (saturated) region in the VLA radio image (Fig. 2, right panel). The VLA image also shows a pair of arms extending up to $5'$ to the east and southwest. The eastern arm appears as a torus atop a stem (a “mushroom cloud”) and represents a buoyant bubble of plasma that has risen about 20 kpc over the past 40-70 Myrs (Owen *et al.* 2000; Churazov *et al.* 2001). Only a twisted filamentary arm remains of the corresponding plasma bubble to the SW. Corresponding X-ray filamentary arms of cool gas, uplifted by the buoyant plasma bubbles, are seen in the Chandra image (left panel). On the largest scales (extending to almost 40 kpc to the north and south), two faint disk-like radio features are probably the remnants of the oldest outbursts from M87 (~ 100 Myrs old; labeled as “outer radio lobe”). The hard band X-ray image (center panel) shows a shock at a radius of $2.8'$ (13 kpc; see also Fig. 4) which is represented in the radio image as a black circle. This shock was produced by a prominent outburst that occurred approximately 12 Myr ago. A surface brightness image in the hard energy band is approximately proportional to the square of the pressure projected on the sky for gas temperatures of 1 - 3 keV (see Churazov *et al.* 2016; Arévalo *et al.* 2016). Images in this band show direct evidence for outbursts as over-pressured, bright regions. The cool filamentary arms, so prominent in the softer band (left panel), are not seen in the hard band and are, hence, in pressure equilibrium with the surrounding plasma.

We use deep Chandra observations of M87, along with a model for the shock observed at a radius of 13 kpc that is being driven by the expansion of the cavity as it is being inflated with relativistic radio-emitting plasma by the SMBH, to derive the properties of the AGN outburst that created the shock. The age of the outburst, giving rise to the shock, is about 12×10^6 years. With the Chandra and radio observations, we can chronicle outbursts from the M87 supermassive black hole over the past 150 Myr.

The 13 kpc shock in M87 was the first classical shock found in the hot gaseous atmosphere around a central cluster galaxy, where both the gas density and gas temperature jumps could be accurately measured. The gas temperature and density jumps are both consistent with the Rankine-Hugoniot shock jump conditions. Fig. 4 shows the projected and deprojected X-ray surface brightness profiles for M87 in the Chandra “hard” (3.5 - 7.5 kev) band (in red) and “soft” (1.2 - 2.5 keV) energy band (in blue).

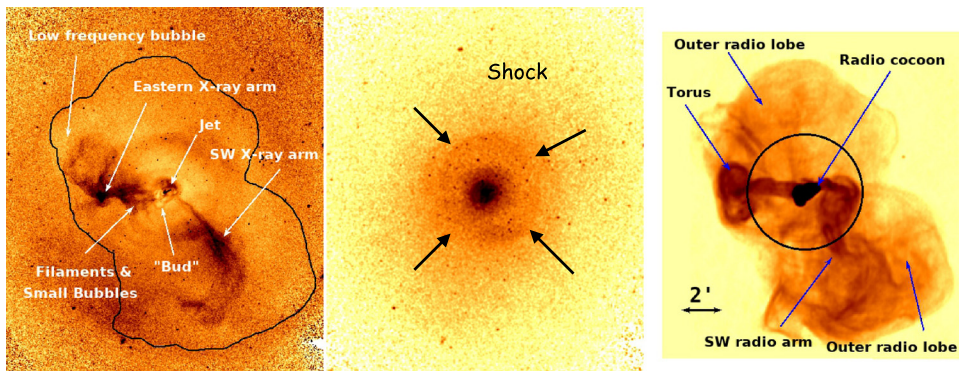


Figure 2. The Chandra broad (left) and hard (center) band images and the 90 cm VLA (right) image, matched in scale, document the major outbursts from M87 (for details see Churazov *et al.* 2001; Forman *et al.* 2007, 2017; Owen *et al.* 2000). (left) Chandra broad band image (0.5–2.5 keV) divided by the average radial profile to show faint surface brightness features. A contour of the faintest surface brightness regions of the radio emission is included. (center) Arrows denote the shock location in the hard band (3.5–7.5 keV) image. (right) The VLA image shows the prominent arms, torus, and outer lobes. The circle shows the location of the X-ray observed shock.

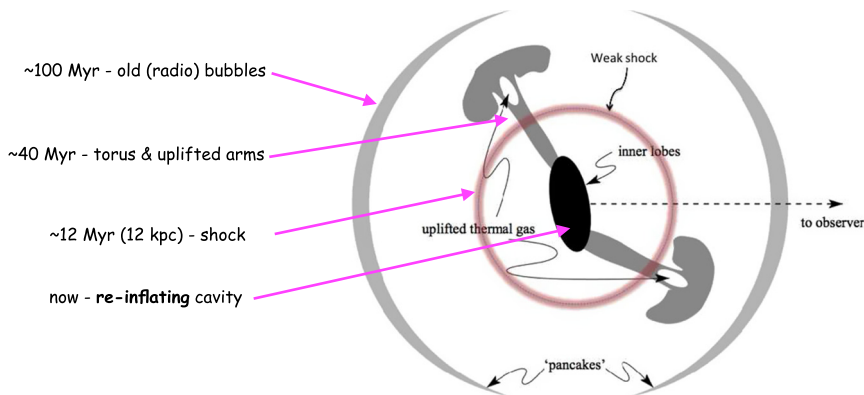


Figure 3. Schematic of M87 activity over the past 100 Myr as chronicled in the radio and X-ray observations. The sketch (adapted from Churazov *et al.* (2001)) shows the oldest outbursts as flattened pancakes, high in the atmosphere, the mushroom shaped tori (one now disrupted), the X-ray shock, and the central cavity that drove the 12 Myr old shock and is now re-pressurizing.

To characterize the outburst properties, simulations were carried out that capture the key physics. The radio plasma, ejected by the jet from the SMBH, inflates a central cavity. The inner radio lobes act as a piston that displaces the hot X-ray gas and drives a shock. By varying the outburst energy and timescale (see Fig. 5), we constrain the outburst parameters and derive the outburst energy, the outburst age, and the outburst duration. Our fiducial model that best characterizes the M87 outburst has an age of 12 Myrs, a total outburst energy of 5.5×10^{57} ergs, and a duration of ~ 2 Myr. At the current time, the shock is expanding at Mach 1.2. By characterizing the outburst, we are also able to derive the energy partition of the outburst. The buoyant bubbles contain the largest fraction of the outburst energy. The initial shock contains $\sim 30\%$ of the outburst energy of which 10% is deposited in shocked gas by the present epoch. The remaining shock energy is carried to large radii as the shock continues to weaken. About 80% of the outburst energy is available for heating the gas in the X-ray bright core.

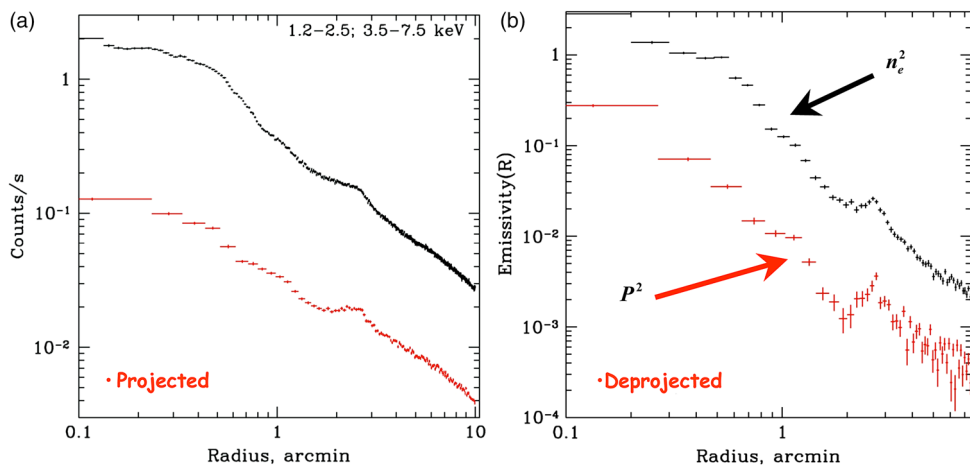


Figure 4. (a) The azimuthally averaged (projected) radial profiles to the north of M87 in the 1.2-2.5 keV (upper curve; mostly sensitive to density) and 3.5-7.5 keV (lower curve; sensitive to pressure) bands; these show a sharp edge at $0.60'$ (most distinctly seen in the hard band as a decrease between the fourth and fifth data points), a moderate flattening of the profile at about $1'$, and a strong excess at $2' - 3'$. (b) The deprojected emissivity profiles, derived from the azimuthally averaged surface brightness profiles in the two energy bands 1.2 - 2.5 keV (upper curve) and 3.5 - 7.5 keV (lower curve). The deprojection shows the very pronounced feature at $2' - 3'$, which represents the 13 kpc shock. In addition, for a spherical shock one expects a rarefaction region trailing the shock front characterized by a density and temperature decrease below the upstream values. Such a rarefaction region is probably seen in panel b at $r \sim 1.5' - 2'$, where the emissivity shows a clear depression.

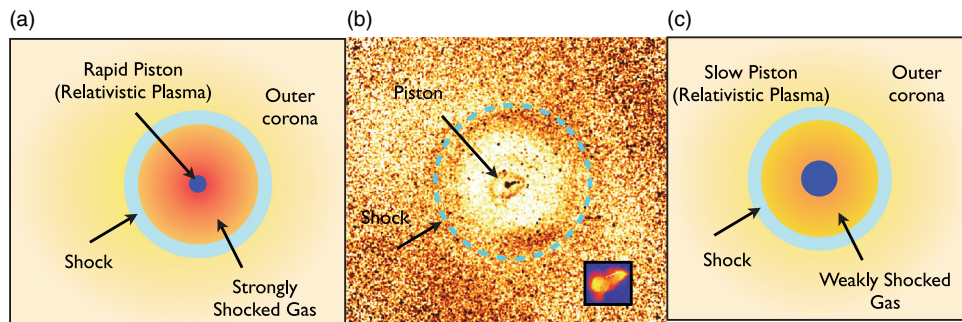


Figure 5. Two shock scenarios (**a - left**) A strong, short duration outburst ($\Delta t = 0.1 \times 10^6$ yrs) drives a strong shock. At present, the region interior to the shock (located at the observed 13 kpc radius) would encircle a central strongly shocked, hot, low density atmosphere. (**b - center**) X-ray image of M87 divided by the average radial profile shows the central piston, that powered the M87 shock, and the jet (6 cm radio image is inset). The dashed blue circle (labeled “Shock”) indicates the outer edge of the shock, seen as the bright ring of emission. (**c - right**) A longer duration outburst, ($\Delta t = 2.2 \times 10^6$ yrs; the fiducial model) provides the same strength shock at 13 kpc, but only weakly shocked gas interior to the shock location and a larger central plasma-filled, piston. The observed data are not consistent with a short duration outburst.

Fig. 5 shows a cartoon version of two outbursts – one with a short duration and a second with long duration – which characterize the quantitative analysis. A powerful, short duration outburst, in the left panel ($\Delta t = 0.1 \times 10^6$ yrs), drives a strong shock into the surrounding atmosphere. At the present time, the region interior to the shock (located at the observed 13 kpc radius) would enclose a central hot, strongly shocked, low density atmosphere. The right panel pictures a longer duration outburst, ($\Delta t = 2.2 \times 10^6$ yrs;

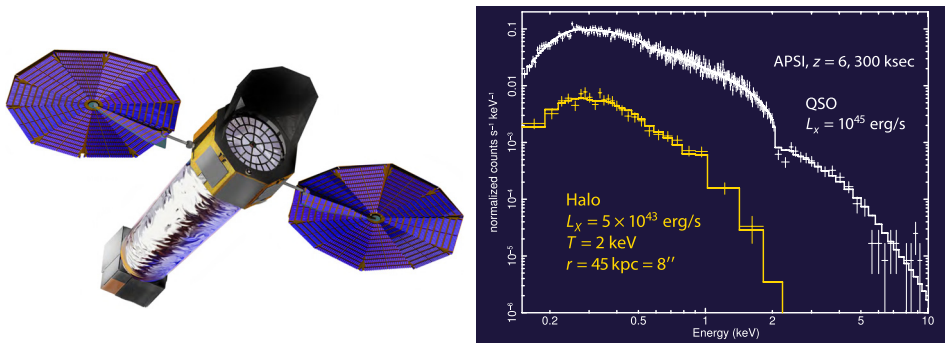


Figure 6. (left) An artist's concept of the Lynx mission that would provide 30 times Chandra's effective area with comparable angular resolution. (right) At redshift $z \sim 6$, Lynx would be able to resolve the bright AGN from its surrounding hot atmosphere and provide a high quality spectrum of the hot atmosphere with a 300 ks observation. With sub-arcsecond angular resolution, Lynx would be able to follow the evolution of hot atmospheres, the dark matter halos in which they are confined, and the AGN, associated with the SMBH at the galaxy nuclei, from high redshift to the present.

referred to as the fiducial model) which provides the same magnitude shock at 13 kpc, but only weakly shocked gas interior to the shock location and a larger central, plasma-filled piston. The central panel shows the actual outburst. The observations do not show a strongly shocked region interior to the shock and the radius of the central cavity matches that observed for our fiducial model with a few Myr duration outburst.

During the subsequent evolution, within the framework of the model, as the buoyant bubble rises, much of its energy is transferred to the ambient cluster gas. For an outburst repetition rate of about 12 million years (the age of the current outburst), 80% of the outburst energy is sufficient to balance the radiative cooling of the gas.

M87 provides a view of a “typical” outburst from a low-Eddington rate accretor with the bulk of the energy liberated as mechanical, rather than radiative, energy with the dominant energy transfer mediated by the buoyant bubbles.

Looking to the future, NASA is studying the Lynx concept, a sub-arcsecond successor to the Chandra X-ray observatory but having 30 times Chandra's area. Such a mission would be able to study the detailed properties of outbursts and probe the conversion of bulk motions to thermal energy (see Fig. 6). Furthermore, the Lynx concept would probe to high redshift with sub-arcsecond angular resolution (Vikhlinin *et al.* 2012, see section 3.1 and Fig. 3) and could fully test models of galaxy evolution and the impact of the SMBHs by studying the AGN and the hot gaseous atmospheres in which they lie. It could trace the evolution of both the AGN and the surrounding hot gaseous atmosphere by deriving their properties (luminosity, temperature, density profile, and abundance) from redshifts of $z \sim 6$ (or higher) to the present.

References

- Arévalo, P., Churazov, E., Zhuravleva, I., Forman, W. R., & Jones, C. 2016, *ApJ*, 818, 14
 Churazov, E., Forman, W., Jones, C., & Böhringer, H. 2000, *A&A*, 356, 788
 Churazov, E., Brüggen, M., Kaiser, C. R., Böhringer, H., & Forman, W. 2001, *ApJ*, 554, 261
 Churazov, E., Sunyaev, R., Forman, W., & Böhringer, H. 2002, *MNRAS*, 332, 729
 Churazov, E., Sazonov, S., Sunyaev, R., *et al.* 2005, *MNRAS*, 363, L91
 Churazov, E., Arevalo, P., Forman, W., *et al.* 2016, *MNRAS*, 463, 1057
 Fabian, A. C., Sanders, J. S., Allen, S. W., *et al.* 2003, *MNRAS*, 344, L43
 Finoguenov, A., & Jones, C. 2001, *ApJ*, 547, L107
 Ford, H. C., Harms, R. J., Tsvetanov, Z. I., *et al.* 1994, *ApJ*, 435, L27

- Forman, W., Nulsen, P., Heinz, S., *et al.* 2005, *ApJ*, 635, 894
Forman, W., Jones, C., Churazov, E., *et al.* 2007, *ApJ*, 665, 1057
Forman, W., Churazov, E., Jones, C., *et al.* 2017, *ApJ*, 844, 122
McNamara, B. R., Nulsen, P. E. J., Wise, M. W., *et al.* 2005, *Nature*, 433, 45
Owen, F. N., Eilek, J. A., & Kassim, N. E. 2000, *ApJ*, 543, 611
Vikhlinin, A., Reid, P., Tananbaum, H., *et al.* 2012, *Proc. SPIE*, 8443, 844316
Walsh, J. L., Barth, A. J., Ho, L. C., & Sarzi, M. 2013, *ApJ*, 770, 86